Combining L1 Signals for Improved Sensitivity

Yu Hsuan Chen, Sherman Lo, Per Enge, *Stanford University*
Dennis Akos, *University of Colorado, Boulder*

BIOGRAPHY

Sherman Lo is a senior research engineer at the Stanford University GPS Laboratory. He is the Associate Investigator for the Stanford University efforts on the FAA evaluation of alternative positioning navigation and timing (APNT) systems for aviation.

Per Enge is the Vance D. and Arlene C. Coffman Professor in the School of Engineering at Stanford University and the director of the Stanford GPS Laboratory.

Yu-Hsuan Chen is a Postdoctoral Scholar in GPS Laboratory at Stanford University. He received his Ph. D in electrical engineering from National Cheng Kung University, Taiwan in 2011.

Dennis M. Akos obtained the Ph.D. degree from Ohio University in 1997. He is an associate professor with the Aerospace Engineering Science Department at University of Colorado at Boulder with visiting appointments at Luleå Technical University and Stanford University.

1. INTRODUCTION

Global Navigation Satellite System (GNSS) receiver developers have long sought to achieve higher sensitivity. This is beneficial for both civilian and military users. Improved sensitivity increases availability in urban and indoor environments and provides greater robustness against radio frequency interference (RFI). With the coming of GPS III, users will have new features that can be used to improve sensitivity. GPS III will provide multiple signals on multiple frequencies. These signals can be processed together to improve sensitivity. At GPS L1, a civilian user will have access to L1 C/A as well as L1C pilot and data. Additionally, military user will also have L1 P(Y) and M code. This paper examines combining different L1 signals to improve sensitivity and how to use the combination with other techniques such as extended averaging. The paper demonstrates results using on air data from the Japanese Quasi-Zenith Satellite System (QZSS).

The goal of this phase is to enable and quantify the sensitivity benefits of combining future GPS L1 signals using our GNSS software defined radio (SDR) and broadcast signals. This paper is divided into two major parts. First part provides background on QZSS along with the combination technique and assessment methodology. The body of the paper discusses the data collected for the analysis and examines the resulting sensitivity performance of the combined technique with natural signal degradation and injected simulated noise.

2. BACKGROUND

GPS III will be the first GPS satellites to transmit the L1C signal. This signal consists of a data and pilot channel – $L1C_d$ and $L1C_p$, respectively. Table 1 shows the specifications for L1C, which uses binary offset carrier (BOC) and time multiplexed BOC (TMBOC) modulation, given in [1]. L1C offers several enhancements over L1 C/A and is designed to be interoperable with other international satellite systems such as Galileo [2][3]. Figure 1 shows the spectrum of L1 with the L1C signals (as well as some Galileo signals). The signal design offers several improved capabilities to users. One benefit for civil users is improved multipath performance over the L1 C/A [4][5]. Another key benefit is improved sensitivity. $L1C_p$ allows for extended integration without the need of external aiding data. The extended integration is especially useful for improving acquisition and tracking sensitivity. This paper examines combining the signals to improved sensitivity. While examines and uses the unencrypted signals: L1 C/A and L1C (pilot and data), these results can be extended to users with access to M and P(Y) code.

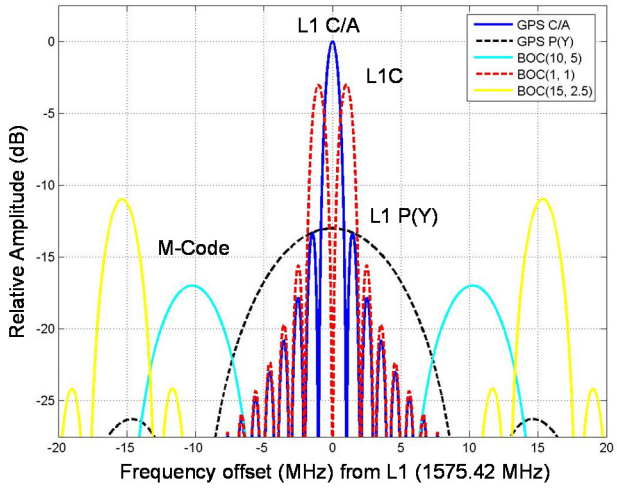

Figure 1. L1 Spectrum with GPS III and Galileo

Table 1. L1C Specifications (GPS III) [1][6]

Signal	L1C pilot	L1C data
PRN (Primary Code) Length	10230	10230
Secondary Code Length	1800 bits per second (bps) (100 bps over 18 sec)	
Modulation	TMBOC: BOC(1,1) + BOC(6,1)	BOC(1,1)
Data rate		50 bps
Symbol rate		100 symbols per second (sps)
Phase	Quadrature	Quadrature
Minimum Received Power (dBW)	-158.25	-163.0
	-157 total on L1C	

We cannot use GPS L1C for our on-air evaluation as there are currently no Block III satellites in orbit. Fortunately, the Japanese Quasi-Zenith Satellite System (QZSS) serves as a good proxy for this study as it has one satellite in orbit and transmits signals comparable to those planned for GPS III: L1 C/A, L1C pilot ($L1C_p$) and L1C data ($L1C_d$) transmissions. There are some slight differences in its L1 transmission when compared to that specified for GPS III. First, the QZSS L1C and L1C/A are offset by 90 degrees (in phase quadrature) whereas these signals on GPS III are in phase. Another signal structure difference is that QZSS L1C is modulated using binary offset carrier (BOC) rather than the time multiplexed BOC (TMBOC) employed on GPS L1C. There are two broadcast difference in the L1 transmissions that is relevant to our study. First, QZSS L1 C/A has a lower specified minimum received signal power than that specified for GPS IIIA L1 C/A. QZSS specifies L1 C/A at -158.5 deciBels (dB) relative to one Watt (dBW) while GPS III specifies -157 dBW. Second, QZSS does not transmit P(Y) or M code.

The specifications for the QZSS transmissions are found in [7]. Table 2 shows the basic characteristics of the L1 signals from the QZSS ICD. One important item for this study is the specified minimum received signal power. L1C pilot is the highest with L1 C/A pretty close. L1C data is the weakest. So the sensitivity results should follow this general order in terms when signal tracking is lost.

Table 2. QZSS L1 Navigation Signals

Signal	L1 C/A	L1C pilot	L1C data
PRN (Primary Code) Length	1023	10230	10230
Secondary Code Length		1800	
Data rate	50 bps		50 bps
Symbol rate	50 sps		100 sps
Phase	In phase	Quadrature	In phase
Minimum Received Power (dBW)	-158.5	-158.25	-163.0
		-157 total on L1C	

Improving Sensitivity

There are many ways to improve GNSS receiver robustness and sensitivity to RFI. Figure 2 shows some of these methods. Antenna-based techniques such as adaptive arrays such (i.e., controlled reception pattern antennas (CRPA)) and high mask angle antennas can improve robustness by creating nulls in regions of incoming RFI. CRPA can also aid sensitivity by increasing gain in the direction of incoming signals.

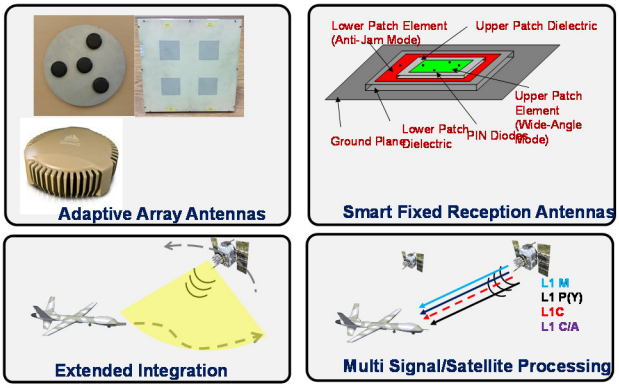

Figure 2. Techniques to Enhance GNSS Robustness

Processing techniques can co-exist with these antenna to further improve sensitivity. Extended integration is extremely powerful and is now commonly employed especially when enabled by assistance data. For example, by extending integration periods from 10 milliseconds (ms) to 100 ms, a nearly tenfold improvement (10 decibels or dB) in signal power may be achieved. Noise power is also increased but not at the same rate.

A final class of processing techniques involves leveraging multiple signals and satellites. Traditional GNSS processing used independent channels for satellites and signals. This class of techniques combines measurements from different satellites and signals to aggregate signal power. For these class of techniques, the processing channels are thus dependent. One example is vector processing which leverages signals from multiple satellites to aid sensitivity [8]. Indeed, the combining signals discussed in this paper could utilize some of the ideas from vector tracking.

Combining multiple signals from the same satellite can be reasonably done by utilizing the coherence between the signals [9][10]. The combination is even easier when the signals are on the same frequency as time varying biases between signals on different frequencies do not need to be estimated. Significant work has been done assessing combining modernized GNSS signals containing a pilot and data component [11][12][13][14][15]. Combining two equally powerful signals potentially yields 3 dB improvement in received power. In this work, we examine combining multiple signals from the same satellite to

improve tracking. Combining signals should be implemented with extended integration periods. While extended integration is common and powerful, a combined signal technique could add a few more dB in sensitivity. We will also demonstrate the combination implemented alongside extended integration.

Stanford Software Defined Receiver

Stanford University (SU) has developed a real-time GNSS software defined radio (SDR) code base capable of supporting multiple constellations (GPS, Galileo and Beidou), multiple signals (L1 C/A, L1C, E1 OS and L5) and multiple antenna inputs (CRPA processing) [16]. This software receiver was modified to implement combined signal tracking with extended integration

The implemented combined tracking approach is based on the work presented in [17]. The technique is illustrated in Figure 3. The technique is selected because it is reasonably straight-forward and can be implemented in our SDR without significant modification. The SDR individually correlates to each signal (L1 C/A, $L1C_p$, $L1C_d$). The correlation sums multiplied by weights (A, B, C) proportional to the relative signal power between each signal. For example, if we combine two signals with one signal having twice the signal power of the other, then we would weigh that signal with twice the weight of the weaker signal. For our implementation, we set A, B, C equaled to 1, 3, and 3, respectively. This is close to but not exactly the ratio based their specified minimum received power. Correlation sums over an interval without bit transitions from each signal are combined. For the analysis, we used 10 milliseconds (ms) as the nominal interval. $L1C_d$ has 100 symbols per second (sps) so 10 ms is the longest time period between symbols. As the bits on the different signals can have different relative signs, all possible sign combinations are calculated. It is assumed that the correct combination is the one with the maximum resultant energy. That result is then fed to code and carrier tracking loop. The carrier uses the in-phase (I) and quadrature (Q) results.

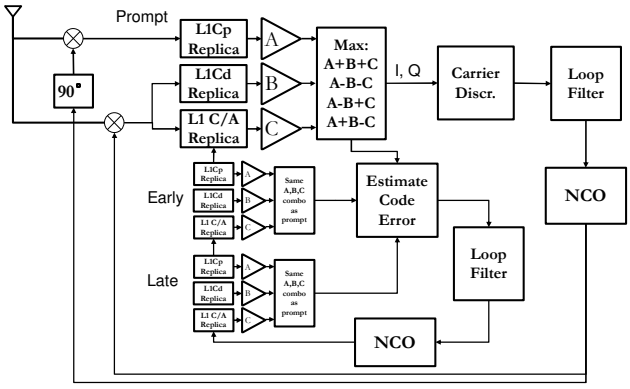

Figure 3. L1 Combined Signal Processing based on [17]

For extended integration, the correlation and summing process are conducted over several bit transitions. Essentially the correlation sums are calculated at every potential bit transition of any of the signal (hence every 10 ms). The maximum value is determined and stored. The maximum values over the integration period are then added in a moving average and used to provide input to the code and carrier tracking loop.

Correlating the maximum amount of signal between bit/symbol transitions leverages the capabilities of a SDR and is illustrated in Figure 4. For each symbol epoch (10 ms), the SDR takes a segment that contains the full current symbol and correlate with a replica of the chips in the current symbol. To guarantee that a full symbol is contained, the segment contains more than 10 ms of data – we used 20 ms. As a result, this segment will overlap with the segment used in the next and previous epochs. For each epoch, we determine the mostly likely relative signs (bits) between the different signals as was done in the nominal case. The correlation sum with the combined power is then summed with results from previous symbol epochs. This process is repeated for the next symbol epoch.

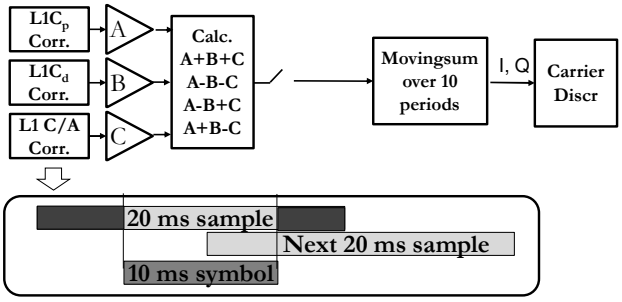

Figure 4. Correlating to each symbol

3. DATA COLLECTION, PROCESSING

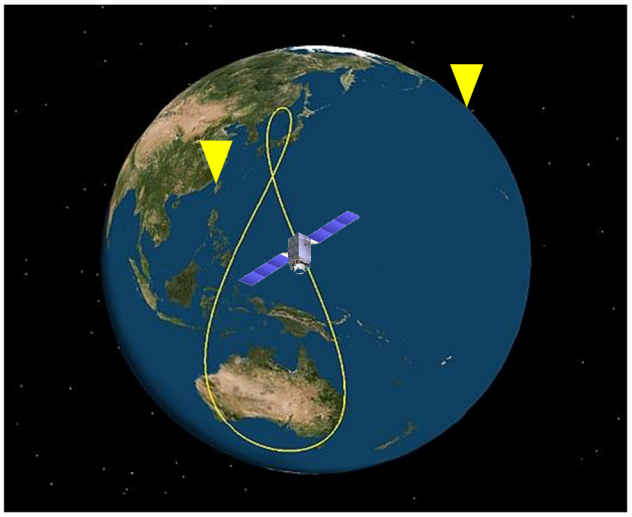

Figure 5. QZS-1 Ground footprint and Data Collection Sites Used in Study

Data was collected at two locations to assess the performance of the developed techniques with on-air signals means. There is currently one QZSS satellite in orbit, Quazi-Zenith Satellite 1 (QZS-1), and it provides coverage for East Asia. It is continuously visible in East Asian countries such as Japan, Taiwan. It is also visible for about 1.5 hour each day at Stanford University in California. Data was collected in Tainan, Taiwan (National Cheng Kung University or NCKU) and California (Stanford University) to be processed using the SU SDR. Figure 5 shows the ground trace of the orbit of QZS-1 as well as the location of the two data collection sites. Figure 6 shows the skyplot of two data collection locations.

A Universal Software Receiver Peripheral (USRP) N210 was used to collect raw I and Q samples for processing by the SU SDR. The USRP collects 14 bits samples and, for our test, a 20 Mega samples per second (Msps). This is the same data collection set up used in [4][5].

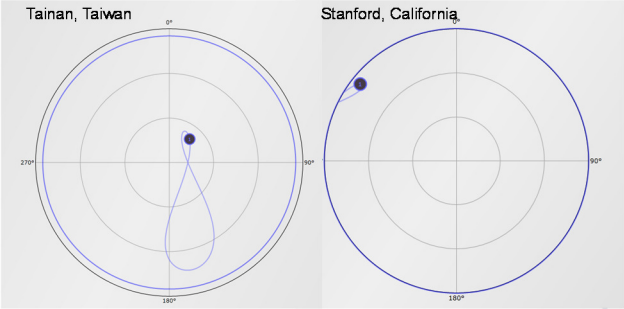

Figure 6. Skyplot of QZS-1 in Tainan, Taiwan and Stanford, California

Figure 7. Stanford Data Collection Set Up on Durand Building

Additionally, the SDR can simultaneous track a given satellite signal at up to five multiple correlator spacings in real time. A standard early minus late correlator tracking is employed. The correlator spacings used in this study are: 0.1, 0.15, 0.2, 0.25, 0.3 chips based on a C/A code chip. For 0.1 chips, the early and late correlators are separated by 0.1 chip from the prompt correlator. So they are 0.2 chips apart. Each correlator spacing is tracked individually and outputs separated range measurement. The SDR outputs at a 10 Hertz (Hz) rate.

The data collected was processed by the SU SDR modified to perform the combined processing of QZSS L1 signals as well as processing the each L1 signal independently. Hence, we get four outputs: L1 C/A, $L1C_p$, $L1C_d$, and Combination. Additionally, both nominal and extended integration versions were implemented with nominal using 10 ms and extended using 100 ms integration intervals.

For this evaluation, we primarily focused on the data collected at Stanford University. Stanford data collection location on the roof of the Durand building is shown in Figure 7. The NCKU data was used to validate the signal combination. However, as the signal was collected at high gain, not enough noise could be added to induce loss of tracking before saturating the 14 bit samples.

Theoretical Gain

Before examining the results, we conducted a simple theoretical analysis of sensitivity gains. Given the specified minimum received power, the theoretical received power of the combination is determined and the gain of the combination relative to different signals is calculated. This is presented in Table 3. The maximum expected gain using the combination on GPS IIIA is 3 dB when compared to L1 C/A only on GPS IIIA. The gain is about 0.8 dB (at 3.8 dB) more on QZSS as QZSS L1 C/A has a lower specified minimum received power. The theoretical gain calculated assumes that the signals are received at the same relative signal powers given by the minimum received power specification.

Table 3. Theoretical Gain of Combining Signals

System	GPS IIIA	QZSS	QZSS/GPS	QZSS/GPS
Signal	L1 C/A	L1 C/A	L1C pilot	L1C data
Minimum Received Power (dBW)	-157	-158.5	-158.25	-163.0
Theoretical Max Gain (dB) of Combined	3	3.8	3.6/4.3	8.3/9

4. EVALUATION OF SENSITIVITY

We employed two methods to evaluate the sensitivity benefits of combining L1 signals with on-air transmissions. Sensitivity is examined by decreasing the carrier to noise ratio (C/No) and determining when signal lock is loss. The loss is evidenced by a drop in C/No or large phase errors with a tracking metric is used to give a precise value. The first way to reduce C/No is use natural attenuation from satellite setting. The second method is to inject noise into the collected data to see when signal tracking is loss. Since artificial noise is injected in this method, we can run this test several times using different noise input. This is

important as tracking loss is a statistical process due to the randomness of noise. So several runs are conduct with the different random seeds for noise to get a statistical sample.

The data used for these two evaluations can come from the same satellite pass. Figure 8 shows the C/No of the tracked signals for an entire pass. The main part of the pass, the signal strength is relatively constant and this is used for our assessment using injected noise. The setting satellite scenario occurs at the end of the pass.

In the figure, 0.15 chip correlator spacing is used. The difference between L1 C/A, $L1C_p$, $L1C_d$ and the L1 Combination is visible during the pass. The combination has C/No slightly higher than $L1C_p$ which is a bit higher than L1 C/A and $L1C_d$. This is the expected order though the difference in C/No do not match the theoretical values.

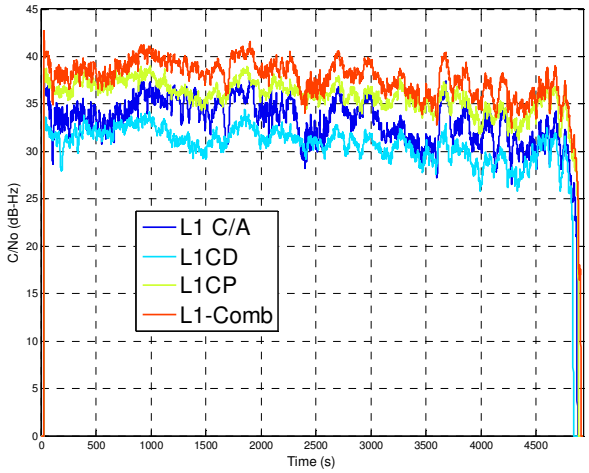

Figure 8. Tracking C/No over QZSS pass at 0.15 chip

Setting Satellite

First, we look at the setting satellite case. Figure 9 zooms in on the last segment of the pass where the satellite is setting for two different correlator spacings. The results are in line with expectation with the order of signal tracking loss: starting with $L1C_d$, then L1 C/A, $L1C_p$, and finally L1 Combination. The trends follow expectation for different correlator spacings and the figure shows the results for two correlator spacings (0.2 and 0.3 chips).

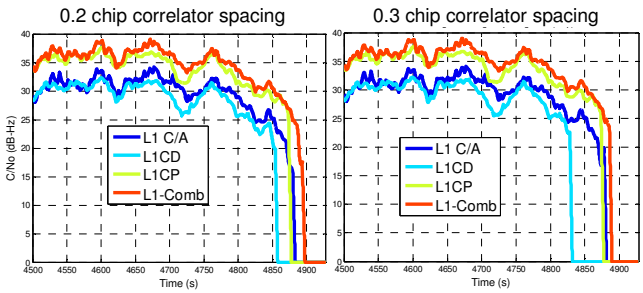

Figure 9. Tracking C/No at end of QZSS pass, 0.2 chip (Left) and 0.3 chip (Right)

Noise Injection

Noise is added to the QZSS data to evaluate and quantify the sensitivity improvement. The noise is added in steps. A stair step function is used so that the receiver has time to settle after the noise level has been increased. Because of the statistical nature of the noise, the receiver may not immediately lose lock upon an increase in noise level. Hence, we let the noise level remain fixed for some time.

For the initial analysis using nominal integration period of 10 ms, the noise was added in steps of 1.5 dB every 30 seconds.

The Stanford data was collected at a lower C/No and a lower gain setting to allow for the addition of more noise prior to saturation. As a result, it was used as the primary source for the analysis.

Figure 10 shows the result for Stanford using our nominal (10 ms) integration for 0.2 chip correlator spacing. Tracking is lost roughly when the C/No drops precipitously (below 20 dB-Hz) indicating loss of lock. The results follow expectation with L1 C/A performing similar to $L1C_p$, and the combined being better than both by a few dB. Figure 11 shows the corresponding phase error for each signal. L1 Combination had better performance for all correlator spacing. There are some cases where, for example, the combined and $L1C_p$ loses tracking at about the same time. This is due to how the noise time series interacts with the tracking. The same injected noise levels but with a different time history can have a different effect. Hence, we analyze the performance statistically using multiple noise time series.

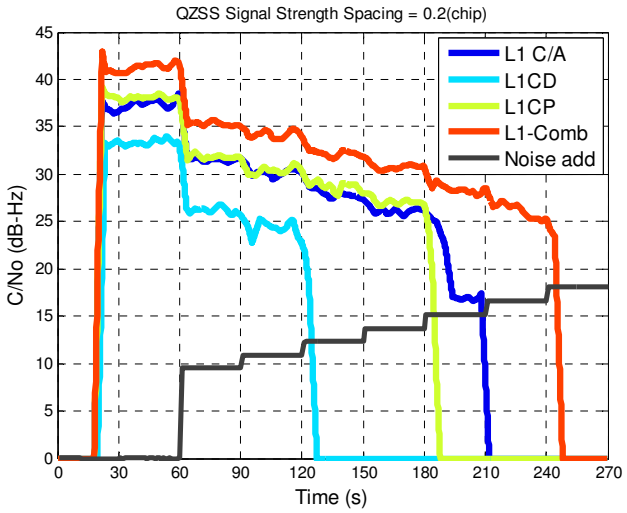

Figure 10. Tracking C/No versus Noise Added for QZSS tracking at 0.2 chip

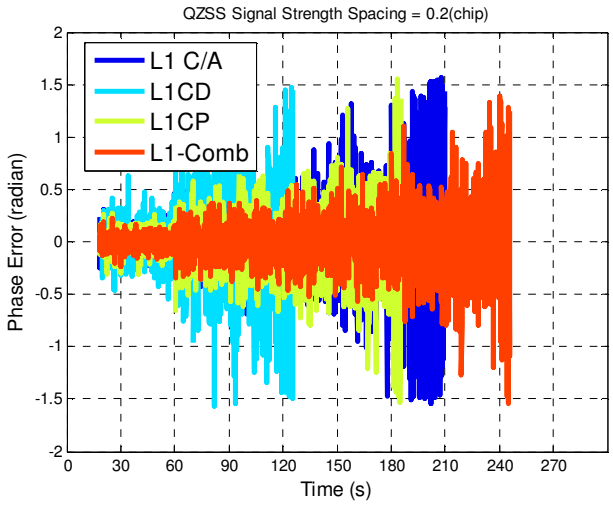

Figure 11. Phase Error with Added Noise

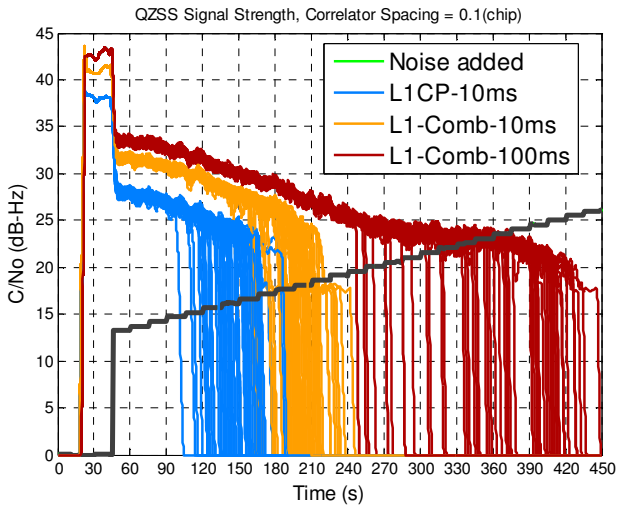

Figure 12. Tracking C/No versus Noise Added for QZSS tracking at 0.15 chip

For the analysis, it is important to have a metric for deciding loss of lock. It is not clear from either Figure 10 or Figure 11 exactly when tracking is lost. We used the cosine of two times the prompt correlator phase, as suggested in [18], as a metric for determining loss of lock. This is readily calculated from the prompt in phase and quadrature sums. A threshold level of 0.2 is used to decide if tracking is locked. If the metric is greater the threshold, then we have tracking. The threshold is set by extrapolating a curve from [18] to our anticipated receiver tracking limit of 18 decibel-Hertz (dB-Hz).

$$\cos(2\varphi) = \frac{|\Sigma I_p|^2 - |\Sigma Q_p|^2}{|\Sigma I_p|^2 + |\Sigma Q_p|^2} > 0.2 \quad (1)$$

Statistical Analysis

A statistical analysis was conducted to assess the sensitivity gain of the signal combination. The noise injected data sets were generated using the same collected on-air data with different noise time series. For each time series set, the noise steps and levels used were the same but different seeds were used to initialize the random function generating the noise. These noise injected data sets were then processed on the SU SDR. These effect of these different noise sets on tracking is shown in Figure 12. The figure shows the tracking performance for each run and one can see that even though the noise level may be the same, there is variation in when the tracking is lost. Using our metric, a histogram of the noise added until loss of tracking for L1 C/A, L1C$_p$ and L1 Combination is generated. Figure 13 shows the results for many runs using our nominal integration (10 ms) period. A different noise set function is used to get more resolution and range. The latter is needed to support evaluation of extended integration. Noise steps of 0.5 dB every 15 seconds was used.

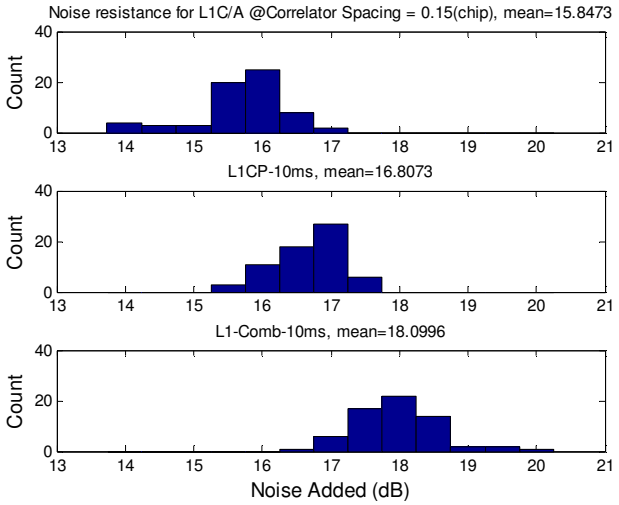

Figure 13. Noise Added until QZSS loss of tracking lock (0.15 chip) (65 trials)

The timing of the tracking loss changes slightly with different correlator spacing. Table 4 shows the mean and standard deviation of the amount of noise that needed to be added to result in loss of lock based on metric. 65 trials were conducted to generate these statistics. As seen in the table, L1 C/A shows the most sensitivity to correlator spacing with its mean sensitivity gain increasing and the standard deviation decreasing with increasing correlator spacing. This is likely primarily due to the interaction of correlator spacing and noise. Noise should have a greater effect on narrower correlator spacing. This effect is not evident for L1C$_p$ and L1 Combination. As a result, the mean sensitivity gain of L1 Combination over L1C$_p$ are generally similar between the chip spacings used. However, it deviates from theory which anticipates 3.5775

dB improvement of L1 Combination over L1C$_p$ based on the minimum specified received power.

Table 4. Mean and Standard Deviation of Noise Added Cause Loss of Lock (65 trials, results in dB)

Chip spacing	0.1	0.15	0.20	0.25	0.30
L1 C/A	15.20	15.85	16.14	16.40	16.37
	0.74	0.70	0.55	0.46	0.48
L1C$_p$	16.27	16.81	16.61	16.64	16.49
	0.61	0.50	0.57	0.62	0.69
L1 Combined	18.04	18.10	18.10	18.12	17.99
	0.65	0.63	0.53	0.50	0.49

Extended Integration

Extended integration was implemented on the SU SDR and tested. Figure 14 shows an example result using 0.15 chip spacing.

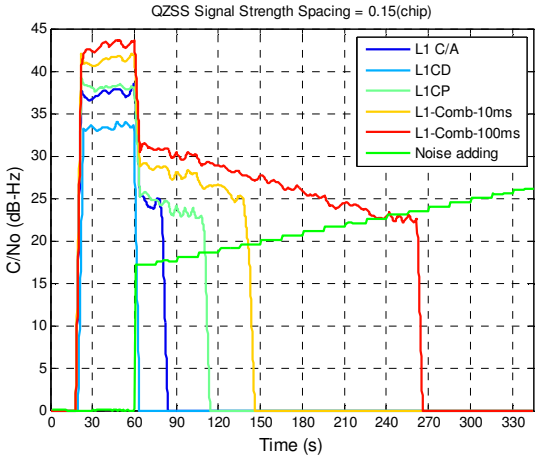

Figure 14. Tracking C/No (with extended integration) versus Noise Added for QZSS tracking at 0.15 chip

As shown previously in Figure 12, multiple runs are conducted and the statistics of the sensitivity gain is tabulated. Figure 15 shows the histogram of the noise added until loss of tracking for L1C$_p$ and L1 Combination, both with 100 ms extended integration. Table 5 presents the statistics of noise added until loss of tracking for extended integration. For L1C$_p$ and L1 Combination, there is slight variation between different correlator spacings but no general trend. Table 6 shows the mean and standard deviation of the sensitivity gain (additional noise needed until loss of tracking) relative to L1C$_p$. As indicated before, the combination seems to have approximately 1.8 dB of improvement. However, if we examine the difference between extended integration implementation of L1 Combination and L1C$_p$, the gain is greater at about 2.8 dB. Additionally, the results show that with extended integration, 4 to 5.5 dB of gain beyond the nominal integration is achieved. This gain is for a tenfold increase in integration time. The L1 Combination with extended integration demonstrated a gain of approximately 7 dB over nominal L1C$_p$ and 7-8 dB over L1 C/A.

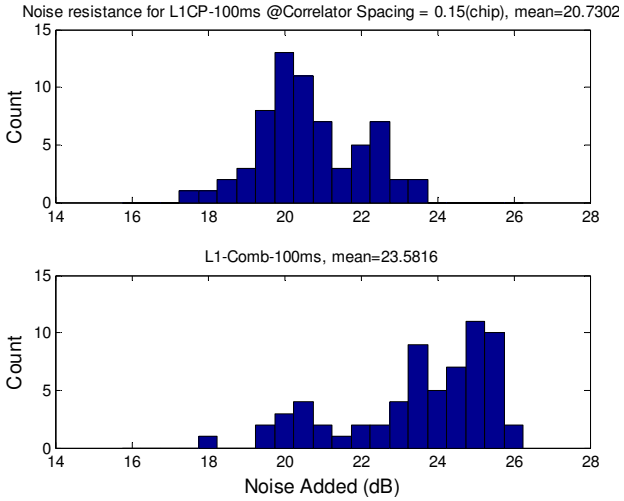

Figure 15. Noise Added until QZSS loss of tracking lock (0.15 chip) for extended integration (65 trials)

Table 5. Mean and Standard Deviation of Noise Added Cause Loss of Lock (65 trials, results in dB)

Chip spacing	0.1	0.15	0.20	0.25	0.30
L1C$_p$ Extended	20.63	20.73	20.51	20.33	20.42
	1.28	1.32	1.22	1.19	1.28
Combined Extended	23.48	23.58	23.66	23.37	23.02
	1.83	1.95	1.76	1.80	1.97

Table 6. Mean Sensitivity Gain (Additional Noise to Lose Lock) Relative to L1C$_p$, 10 ms (65 trials, results in dB)

Chip spacing	0.1	0.15	0.20	0.25	0.30
L1 C/A	-1.07	-0.96	-0.48	-0.25	-0.13
Combined	1.77	1.29	1.49	1.48	1.50
L1C$_p$ Extended	4.36	3.92	3.90	3.69	3.93
Combined Extended	7.21	6.77	7.04	6.73	6.53

The simultaneous use of extended integration and combined signals is an important demonstration. From the previous results, the benefits seem to be additive. This is important as there are limits to extended integration – it cannot be extended indefinitely. The phase error and estimated Doppler frequency are show in Figure 16 and Figure 17. Figure 16 shows the phase error growing large, starting with the initial injection of 17 dB of noise. The combination with extended integration has the least amount of phase noise. However, prior to losing lock, its error regularly exceed a radian. Figure 17 shows that frequency is reasonably tracked by the L1 Combination with extended integration up to the point of losing lock.

The receiver phase lock loop essentially reverts to being frequency lock loop.

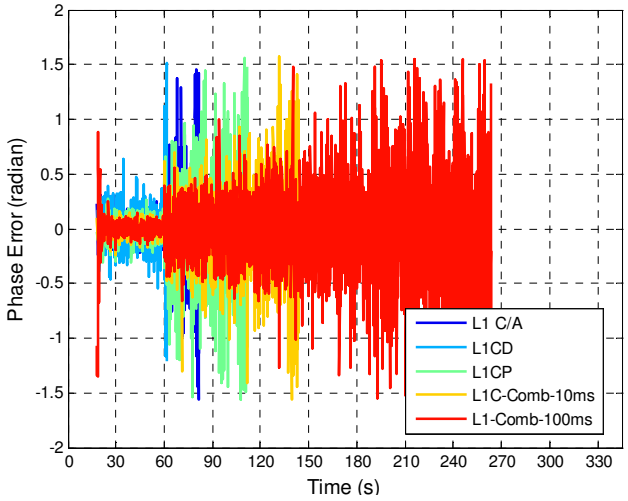

Figure 16. Tracking Loop Phase Error with Injected Noise

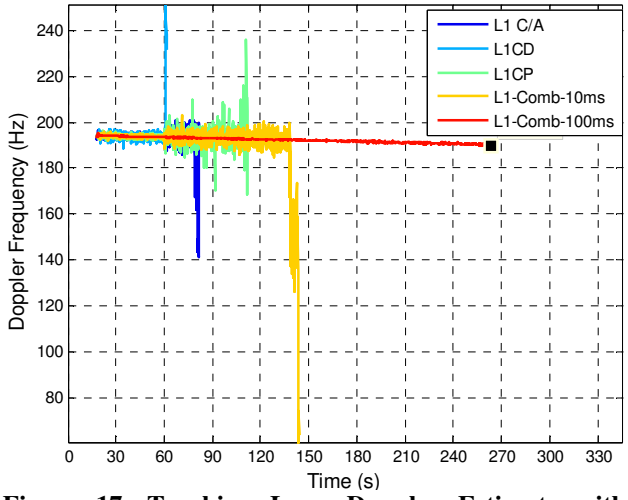

Figure 17. Tracking Loop Doppler Estimate with Injected Noise

So while extended integration will allow us to track with significant noise, it will have large phase error. Having both extended integration and the combined signal technique allows for further sensitivity improvements over each alone, allowing for tracking in the presence of more noise or reduction of phase or frequency error over using just one of the techniques alone.

5. CONCLUSIONS

This work implemented combined tracking of QZSS L1 signals in the Stanford software defined receiver. This work also developed and implemented a means of using extended integration technique with the signal combination. This work demonstrated improved tracking sensitivity of both implementations with on-air data with simulated and real attenuation. The results show that the implemented combined signal technique had 1.8 to 2.8 dB improvement over traditional tracking of C/A only. This compares to a theoretical benefit of 3.58 dB. Adding 100 ms of extended integration further improved sensitivity with an additional 4 to 5.5 dB improvement over 10 ms integration period.

The difference between actual performance and theoretical suggests further work and areas of improvement. Several areas will be investigated. One area is relative signal power – this may differ from theoretical. Furthermore, the relative weighting of the signals should adequately reflect the actual. Another area is to examine processing architectures that takes more advantage of the $L1C_p$ signal.

ACKNOWLEDGEMENTS

The authors would like to thank the Stanford Center for Position Navigation and Time (SCPNT) for supporting this work. We thank the MECLAB at NCKU for gathering and providing the QZSS datasets from Taiwan. We also thank Michael Souder at Lockheed Martin for his inputs.

DISCLAIMERS

The views expressed herein are those of the authors and are not to be construed as official or reflecting the views of any other group.

REFERENCES

[1] Global Positioning Systems Directorate Systems Engineering & Integration, "Navstar GPS Space Segment/User Segment L1C Interface Specification IS-GPS-800", IS-GPS-800D, September 2013

[2] J. Betz, M.A. Blanco, C.R. Cahn, P.A. Dafesh, C.J. Hegarty, K.W. Hudnut, V. Kasemsri, R. Keegan, K. Kovach, L.S. Lenahan, H.H. Ma, J.J. Rushanan, D. Sklar, T.A. Stansell, C.C. Wang, S.K. Yi, "Description of the L1C Signal," Proceedings of the 19th International Technical Meeting of the Satellite Division of The Institute of Navigation (ION GNSS 2006), Fort Worth, TX, September 2006, pp. 2080-2091.

[3] J. Betz, M.A. Blanco, C.R. Cahn, P.A. Dafesh, C.J. Hegarty, K.W. Hudnut, V. Kasemsri, R. Keegan, K. Kovach, L.S. Lenahan, H.H. Ma, J.J. Rushanan, D. Sklar, T.A. Stansell, C.C. Wang, S.K. Yi, "Enhancing the Future of Civil GPS: Overview of the L1C Signal," InsideGNSS, Spring 2007

[4] C. Lee, Y.-H. Chen, G. Wong, S. Lo, and P. Enge, "Multipath Benefits of BOC vs. BPSK Modulated Signals Using On-Air Measurements," Proceedings of the Institute

of Navigation ITM Conference, San Diego, CA, January 2013, pp. 742–751.

[5] Y.-H. Chen, S. Lo, D. Akos, P. Enge, "Direct Comparison of L1 BOC(1,1) vs L1 C/A multipath performance Using On Air Galileo and QZSS transmissions," Proceedings of the Institute of Navigation/Institute of Electronics and Electrical Engineers Position Location and Navigation Symposium (PLANS), Monterrey, CA, May 2014

[6] W. Marquis, M. Shaw, "GPS III: Bringing New Capabilities to the Global Community," InsideGNSS, September/October 2011

[7] Japan Aerospace Exploration Agency (JAXA), "Quasi-Zenith Satellite System Navigation Service Interface Specification for QZSS (IS-QZSS)," Version 1.5, March 27, 2013

[8] J. J. Spilker Jr. and F. D. Natali, "Intereference Effects and Mitigation Techniques," from "Global Positioning System: Theory and Applications", Volume I, Edited by B. W. Parkinson, J. J. Spilker Jr. AIAA, 1996

[9] T. H. Ta, M. Pini, L. Presti, "Combined GPS L1C/A and L2C signal acquisition architectures leveraging differential combination," IEEE Transactions on Aerospace and Electronic Systems, 2014

[10] C. Gernot, K. O'Keefe, G. Lachapelle, "Assessing Three New GPS Combined L1/L2C Acquisition Method," IEEE Transactions on Aerospace and Electronic Systems, Volume 47, Issue: 3, 2011

[11] D. Borio, C. O'Driscoll, G. Lachapelle, "Coherent, Noncoherent, and Differentially Coherent Combining Techniques for Acquisition of New Composite GNSS Signals," IEEE Transactions on Aerospace and Electronic Systems, Volume 45, Issue: 3, 2009

[12] C. Yang, C. Hegarty, and M. Tran, "Acquisition of the GPS L5 Signal Using Coherent Combining of I5 and Q5" Proceedings of the Institute of Navigation GNSS Conference, Long Beach, CA, September 2004

[13] K. C. Seals, W. R. Michalson, P. F. Swaszek, R. J. Hartnett, "Analysis of Coherent Combining for GPS L1C Acquisition," Proceedings of the 25th International Technical Meeting of The Satellite Division of the Institute of Navigation (ION GNSS 2012), Nashville, TN, September 2012

[14] J. Zhou, C. Liu, "Joint data-pilot acquisition of GPS L1 civil signal," 12th International Conference on Signal Processing (ICSP), 2014

[15] B.A. Siddiqui, J. Zhang, M. Z. H. Bhuiyan, E. S. Lohan, "Joint Data-Pilot acquisition and tracking of Galileo E1 Open Service signal," Ubiquitous Positioning Indoor Navigation and Location Based Service (UPINLBS), 2010

[16] Y.-H. Chen, J.-C. Juang, J. Seo, D. S. De Lorenzo, S. Lo, P. Enge, D. Akos, "Design and Implementation of Real-time Software Radio for GPS/WAAS Controlled Reception Pattern Antenna Array Adaptive Processing", Sensors (2012), Sensors 2012, 12(10), 13417-13440

[17] J. F. Macchi-Gernot, M. G. Petovello, G. Lachapelle, "Combined Acquisition and Tracking Methods for GPS L1 C/A and L1C Signals," International Journal of Navigation and Observation, Volume 2010, Article ID 190465

[18] A. J. Van Dierendonck, "GPS Receivers", from "Global Positioning System: Theory and Applications", Volume I, Edited by B. W. Parkinson, J. J. Spilker Jr. AIAA, 1996